

Universal low-energy properties of three two-dimensional bosons

O. I. Kartavtsev and A. V. Malykh

Joint Institute for Nuclear Research, Dubna, 141980, Russia

(Received 2 June 2006; published 11 October 2006)

Universal low-energy properties are studied for three identical bosons confined in two dimensions. The short-range pairwise interaction in the low-energy limit is described by means of the boundary condition model. The wave function is expanded in a set of eigenfunctions on the hypersphere, and the system of hyperradial equations is used to obtain analytical and numerical results. Within the framework of this method, exact analytical expressions are derived for the eigenpotentials and the coupling terms of hyperradial equations. The derivation of the coupling terms is generally applicable to a variety of three-body problems provided the interaction is described by the boundary condition model. The asymptotic form of the total wave function at a small and a large hyperradius ρ is studied, and the universal logarithmic dependence $\sim \ln^3 \rho$ in the vicinity of the triple-collision point is derived. Precise three-body binding energies and the $(2+1)$ -scattering length are calculated.

DOI: [10.1103/PhysRevA.74.042506](https://doi.org/10.1103/PhysRevA.74.042506)

PACS number(s): 36.10.-k, 03.65.Ge, 21.45.+v, 34.50.-s

I. INTRODUCTION

The dynamics of a few particles confined in two dimensions (2D) is of interest in connection with numerous investigations ranging from ultracold gases [1–4] to atoms absorbed on a surface [5–7]. An additional motivation is aroused by specific features of quantum systems in 2D [8–10]. Experiments with ultracold gases in the 2D and quasi-2D traps have been recently realized [1,2].

A description of elementary processes in ultracold gases has been attracting great interest in the last years, and many aspects of the low-energy few-body dynamics in 3D have been thoroughly investigated. As a particular important example, one could mention studies of the three-body recombination for spinless bosons [11–14], two-component fermions [15], and particles with internal degrees of freedom in the presence of a Feshbach resonance [16,17]. The low-energy few-body dynamics in low dimensions is less investigated despite extensive studies. Besides, new phenomena and additional complications arise in quasi-low-dimensional geometry if the effect of motion in the transverse directions is taken into account (see, e.g., [3,18–21]). Among different aspects of 2D systems, one should mention the treatment of the three-body energy spectra [22–24], low-energy scattering of an atom off a dimer molecule [25], and low-energy three-to-three scattering [26,27]. The precise binding energy of four bosons was calculated in [28], and the universal law for the N -boson ground-state energy was discussed in [29].

Concerning other 2D and quasi-2D problems, considerable efforts have long been devoted to the investigation of atoms adsorbed on a surface, including helium atoms on graphite [30] and hydrogen atoms on a helium film [5–7]. In this respect, one should mention the observation of a quasi-condensate [6], measurement of the three-body recombination rate [7], and a vast number of theoretical papers—e.g., [10,31,32].

In the low-energy limit, which is of interest both for practical applications and from a general point of view, the description of the few-body system becomes universal—i.e., essentially independent of the details of the two-body inter-

actions. Among different results of this sort, notice the recent analytical derivation of the universal constants for the zero-energy three-boson scattering in 3D [14,33]. The description becomes parameterless if the only parameter describing the two-body interactions—e.g., the two-body scattering length a —is chosen as a scale [34–36]. In comparison with the universal description in 3D, it is of importance that the solutions of the three-body problem in 2D, contrary to the 3D one, remain regular near the triple-collision point even in the zero-range-interaction limit. This regularity implies, *inter alia*, the absence of Thomas and Efimov effects, which was noticed in [8,9]. Thus, there is no additional regularization parameter, which was introduced in 3D, and the three-body properties in 2D are completely determined by the two-body input that provides a completely universal and parameterless description in the low-energy limit. In particular, the trimer binding energies and the $2+1$ scattering length become the universal constants, which must be determined with good accuracy.

The universal limit corresponds to the limit of the vanishing interaction range r_0 so that r_0 must be much smaller than any length scale in the system; i.e., the binding energies do not exceed the characteristic energy $\frac{\hbar^2}{mr_0}$. Practically, the universal limit can be realized by adjusting the parameters of interaction to diminish the two-body binding energy—e.g., by tuning the position of the Feshbach resonance. To approach the universal limit, one could use the dependence on the particle mass; e.g., an interesting way is to study the isotopic effect for 2D helium atoms [22]. Generally, the universal limit in 2D appears for a very weak potential with a nonpositive average as it is known that in this case the two-body binding energy in 2D becomes exponentially small with decreasing potential strength [37]. It is worthwhile to mention a qualitative difference of the universal properties in 2D and 3D; namely, one expects that both three-body bound states arise simultaneously with the two-body bound state—i.e., at the infinite two-body scattering length. This conjecture is supported by the calculations [22,38], which considered the dependence of the three-body binding energy on the particle mass and potential strength in the limit of the van-

ishing two-body binding energy. Recall that in 3D an infinite number of three-body bound states arise with increasing potential strength at finite values of the scattering length before the two-body bound state arises.

In the present paper, the universal properties of three identical 2D bosons are studied within the framework of a method which makes use of the boundary condition model (BCM) [9,39] for the s -wave interparticle interaction. The two-body interaction introduced in this way is known in the literature as the zero-range potential [40], the Fermi pseudopotential [39], and the Fermi-Huang pseudopotential (see, e.g., Refs. [41,42]) and an equivalent approach is used also in the momentum-space representation [28,29,36]. As proposed in Ref. [43], the wave function is expanded in a set of eigenfunctions on the hypersphere and the resulting system of hyperradial equations (HRE's) is used to conveniently treat both the boundary and scattering problem. One of the principal advantages is that for the two-body interaction given by the BCM the eigenpotentials of HRE's are solutions of a simple eigenvalue equation. The aim of the present paper is to derive in analytical form all the terms of HRE's, thus determining the coupling terms via the eigenpotentials and their derivatives over the hyperradius. Both the derivation and expressions found are generally applicable to a variety of problems; the coupling terms can be obtained in analytical form for three particles of arbitrary permutation symmetry, with arbitrary masses and scattering lengths, and for any dimension of the configuration space. In particular, coupling terms of the same analytical form were derived for three bosons [35] and three two-component fermions [53] in 3D. The exact expressions are used to analyze the asymptotic behavior of the total wave function both at large and small interparticle separations; e.g., the universal dependence of the total wave function near the triple-collision point is found.

Until now, numerical calculations of the universal constants have included the early calculation [8] of the binding energies of three 2D bosons by solving the momentum-space integral equations. Much better precision was obtained by solution of the hyperradial equations [23,44], the results of which were not in complete agreement with those of [8]. Up to date, in the universal limit of zero-range interactions the most precise binding energies have been found by solving the momentum-space integral equations [29]. Among scarce studies of the low-energy three-body scattering in 2D, the only available calculation in Ref. [25] demonstrated a smooth dependence of the 2+1 scattering length on the interaction range. In the present paper, the precise universal values of the three-body binding energies and the scattering length for a particle collision off a bound pair are calculated.

It has been known for a long time (see, e.g., [45,46]) that the one-dimensional problem of N identical particles with zero-range interactions (in this case, Dirac's δ function) is exactly soluble. On the other hand, the method of the present paper, including the derivation of the exact expressions for the coefficients of HRE's, is equally applicable to the three-body problem in 1D. Note that the approach based on solution of HRE's was used in Ref. [47] to discuss low-energy 2+1 scattering in 1D. The calculation of the 1D three-body problem provides a good opportunity to test the approach, to

check the numerical procedure, and to compare the 1D and 2D calculations. For these reasons, the main discussion of the 2D three-body problem is complemented by a brief treatment of the corresponding 1D problem.

The paper is organized in the following manner. The next section contains information on the low-energy two-body scattering in 2D, introduces the boundary condition model, and describes the expansion of the wave function in a set of eigenfunctions on the hypersphere. Analytical results are collected in Sec. III, starting with the eigenvalue equation which determines the eigenpotentials for HRE's. Furthermore, analytical expressions for the coupling terms in HRE's are derived. On the ground of these results, the asymptotic form of the eigenpotentials and coupling terms is obtained and applied to derive implications of the asymptotic behavior of the solution of HRE's. The numerical procedure and the results of the numerical calculations are described in Sec. IV, and the last section contains a summary and a final conclusion. The results for three identical bosons in 1D are briefly discussed in the Appendix.

II. METHOD

The present study is aimed at the description of the low-energy properties of three identical 2D bosons with short-range pairwise interaction in the limit of the zero interaction range. The description turns out to be universal—i.e., essentially independent of the details of the two-body interaction. In the low-energy limit under consideration, only the zero total angular momentum $L=0$ should be considered and only the s -wave two-body interaction should be taken into account. The two-body input for the three-body problem is set as the universal low-energy description of the two-body interaction by a single parameter, for which the two-body scattering length a can be suitably chosen. The scattering length in 2D is defined by the asymptotic form of the zero-energy wave function at large interparticle separation r beyond the interaction range, $\Psi \sim \ln(r/a)$ [9,10]. This is analogous to the definition of the scattering length in 3D as the distance at which the asymptotic expression of the wave function crosses zero. Clearly, with this definition the 2D low-energy scattering is the same as the scattering on the hard disk with radius $r_d=a$. The s -wave scattering amplitude, in accordance with the effective-range expansion [10,25,48,49], in the low-energy limit $k \rightarrow 0$ is completely determined by the 2D scattering length a ,

$$f_0(k) = \frac{\sqrt{2i/\pi k}}{\cot \delta_0(k) - i} \approx \sqrt{\frac{\pi i}{2k}} \left[\ln \frac{ka}{2} + \gamma - i \frac{\pi}{2} \right]^{-1}, \quad (1)$$

where k is the wave number, $\delta_0(k)$ is the s -wave scattering phase shift, and $\gamma \approx 0.5772$ is the Euler constant. The three-body 2+1 scattering—i.e., the collision of the bound dimer off the third particle—below the three-body threshold is described in the same way as the two-body scattering. At low kinetic energy of colliding particles, the s -wave (2+1)-scattering amplitude is described by the effective-range expansion of the form (1), where the two-body scattering length a is replaced by the (2+1)-scattering length A and

k denotes the wave number for the relative motion of a dimer and the third particle.

A. Boundary condition model

In the low-energy limit under consideration, a convenient one-parameter description of the two-body interactions is obtained within the framework of the BCM corresponding to the vanishing range of interaction. In this approach, the exact scattering amplitude $f_0(k)$ is determined by the low-energy expression (1) for an arbitrary k and the two-body binding energy equals $\frac{4\hbar^2}{ma^2}e^{-2\gamma}$, which corresponds to the pure imaginary pole of $f_0(k)$ at $ka=i2e^{-\gamma}$. Explicitly, the s -wave boundary condition which provides the above-discussed low-energy behavior can be written [9] as

$$\lim_{r \rightarrow 0} \left[\frac{d}{dr} - \frac{1}{r \ln(r/a)} \right] \Psi = 0. \quad (2)$$

The total interaction of three particles is a sum of two-body potentials, which are replaced in the BCM by the two-body boundary condition of the form (2) for each pair of particles. As the only parameter describing the two-body interactions is the scattering length a , the units $\hbar=m=a=1$ will be used throughout the paper; thereby, the three-body problem becomes parameterless. The total wave function Ψ satisfies the boundary conditions and the Helmholtz equation

$$[\Delta_{\mathbf{x}} + \Delta_{\mathbf{y}} + E]\Psi = 0, \quad (3)$$

where \mathbf{x} and \mathbf{y} are an arbitrary pair of the scaled Jacobi coordinates defined via the particles' radius vectors \mathbf{r}_i as $\mathbf{x}_i = \mathbf{r}_j - \mathbf{r}_k$ and $\mathbf{y}_i = \frac{1}{\sqrt{3}}(2\mathbf{r}_i - \mathbf{r}_j - \mathbf{r}_k)$. Different sets of the Jacobi coordinates are related by $\mathbf{x}_i = -c\mathbf{x}_j + s\mathbf{y}_j$ and $\mathbf{y}_i = -s\mathbf{x}_j - c\mathbf{y}_j$, where $c=1/2$, $s=\pm\sqrt{3}/2$, and the \pm sign is chosen if $\{ijk\}$ is an even or odd permutation of $\{123\}$. The wave function Ψ of three identical particles is symmetrical under any permutation of the particles; therefore, it is sufficient to impose just one boundary condition

$$\lim_{x \rightarrow 0} \left[\frac{\partial}{\partial x} - \frac{1}{x \ln x} \right] \Psi = 0, \quad (4)$$

where x is any of three interparticle distances.

B. Hyperradial expansion

Solution of a system of HRE's provides an efficient approach to treat both the eigenvalue and scattering problem for the three-body system. This approach is particularly advantageous due to the use of the BCM since all the terms of HRE's are expressed in the analytical form [23,35], which allows one to obtain the exact asymptotic form of the wave function and to improve the accuracy of the numerical calculations. The system of HRE's is obtained by expanding the total wave function in a set of eigenfunctions on the hypersphere $\Phi_n(\alpha, \theta, R)$,

$$\Psi = e^{-R} \sum_{n=1}^{\infty} f_n(R) \Phi_n(\alpha, \theta, R), \quad (5)$$

where the hyperspherical variables ρ ($0 \leq \rho < \infty$), α_i ($0 < \alpha_i \leq \pi/2$), and θ_i ($0 < \theta_i \leq \pi$) are introduced by the relations

$x_i = \rho \sin \alpha_i$, $y_i = \rho \cos \alpha_i$, and $\cos \theta_i = (\mathbf{x}_i \mathbf{y}_i) / x_i y_i$ and $R = \ln \rho$ is a convenient variable in 2D. Different sets of hyperspherical variables are related by $\cos 2\alpha_i = -c \cos 2\alpha_j + s \sin 2\alpha_j \cos \theta_j$ and $\sin 2\alpha_i \cos \theta_i = \pm s \cos 2\alpha_j - c \sin 2\alpha_j \cos \theta_j$. By definition, $\Phi_n(\alpha, \theta, R)$ are regular solutions of the eigenvalue problem on the hypersphere—i.e., at fixed R —deduced from Eqs. (3) and (4):

$$[\Lambda^2 + \xi_n^2(R) - 1]\Phi_n(\alpha, \theta, R) = 0, \quad (6)$$

$$\lim_{\alpha \rightarrow 0} \left[\frac{\partial}{\partial \alpha} - \frac{1}{\alpha(R + \ln \alpha)} \right] \Phi_n(\alpha, \theta, R) = 0, \quad (7)$$

where

$$\Lambda^2 = \frac{\partial^2}{\partial \alpha^2} + 2 \cot 2\alpha \frac{\partial}{\partial \alpha} + \frac{4}{\sin^2 2\alpha} \frac{\partial^2}{\partial \theta^2}. \quad (8)$$

Like the total wave function, the functions $\Phi_n(\alpha, \theta, R)$ are symmetrical under any permutation of particles; i.e., $\Phi_n(\alpha, \theta, R)$ are independent of the index enumerating the Jacobi coordinates.

For each value of the variable R , the problem (6) and (7) determines an infinite number of discrete eigenvalues $\xi_n^2(R)$ and corresponding eigenfunctions Φ_n normalized by the condition $\langle \Phi_n | \Phi_m \rangle = \delta_{nm}$. Henceforth the notation $\langle \cdot | \cdot \rangle$ means integration over the invariant volume on the hypersphere, $d\Omega = \frac{1}{12} \sin 2\alpha d\alpha d\cos \theta$, where the arbitrarily chosen factor $1/12$ is suitable for the derivation of the coupling terms in Sec. III B. The expansion (5) of the total wave function leads to a system of HRE's which can be written in two equivalent forms

$$\left[-\frac{d^2}{dR^2} - \mathbf{Q}(R) \frac{d}{dR} - \frac{d}{dR} \mathbf{Q}(R) + \mathbf{U}(R) + \mathbf{P}(R) - Ee^{2R} \right] \mathbf{f}(R) = 0, \quad (9)$$

$$\left[-\left(\frac{d}{dR} + \mathbf{Q}(R) \right)^2 + \mathbf{U}(R) - Ee^{2R} \right] \mathbf{f}(R) = 0, \quad (10)$$

where $\mathbf{f}(R)$ is the vector function composed of the hyperradial channel functions $f_n(R)$ and the matrices of eigenpotentials $\mathbf{U}(R)$ and coupling terms $\mathbf{Q}(R)$ and $\mathbf{P}(R)$ are defined by their matrix elements

$$U_{nm}(R) = \xi_n^2(R) \delta_{nm}, \quad (11)$$

$$Q_{nm}(R) = \langle \Phi_n | \Phi'_m \rangle, \quad (12)$$

$$P_{nm}(R) = \langle \Phi'_n | \Phi'_m \rangle, \quad (13)$$

with the prime denoting the derivative over R . The identity

$$P_{nm} = \sum_{k=1}^{\infty} Q_{nk} Q_{mk} \quad (14)$$

provides the equivalence of the infinite systems of equations in the forms (9) and (10).

Although two infinite systems of HRE's (9) and (10) are equivalent, the truncated ones give rise to different results,

which allows one to estimate convergence with increasing number of HRE's, N , in practical calculations. Notice that N HRE's of the form (9) reduce to the form (10) if the N -dimensional matrix $\mathbf{P}^{(N)}$ is replaced by a product of N -dimensional matrices $\mathbf{Q}^{(N)}$, $\mathbf{P}^{(N)} \rightarrow -\mathbf{Q}^{(N)}\mathbf{Q}^{(N)}$. It is important that the solution of the truncated system of N HRE's taken in the form (9) gives the upper bound $E_i^{(N)}$ for the exact energy of the i th state E_i and the upper bound $A^{(N)}$ for the exact $(2+1)$ -scattering length A —i.e., $E_i^{(N)} \geq E_i$ and $A^{(N)} \geq A$ [50,51]. The proof can be obtained by observing that the truncated system of HRE's in the form (9) can be obtained by application of the variational principle with the trial function containing a finite sum of the form (5). On the other hand, the solution of HRE's (10), at least in the one-channel approximation, gives the lower bound for the ground-state energy [50]. Solution of the system (9) generally provides faster convergence with increasing number of equations, while solution of the system (10) does not require elaborate calculation of $P_{nm}(R)$. Notice that the scattering length can be calculated by solving only the truncated system (9) because the first-channel effective potential $U_1^{eff}(\rho)$ decreases as $1/\rho^4$ (see Sec. III C). In contrast to that, the first-channel effective potential in the truncated system (10) is of the form $U_1^{eff}(\rho) = [\xi_1^2(\rho) + \sum_{n=1}^N Q_{1n}^2(\rho)]/\rho^2$ and contains a long-range term $\sim -1/3\rho^2$ for any finite N , which prevents calculation of the scattering length.

III. ANALYTICAL RESULTS

A. Eigenvalue problem on the hypersphere

It is convenient to take account of the permutation symmetry and to satisfy the boundary condition (7) by means of the Faddeev-like decomposition

$$\Phi(\alpha, \theta, R) = \sum_{i=1}^3 \chi(\alpha_i, R), \quad (15)$$

provided the function $\chi(\alpha_i, R)$ is symmetrical under the permutation of the particles j and k and satisfies the same equation on a hypersphere (6) as the eigenfunction $\Phi(\alpha, \theta, R)$. The representation (15) is advantageous due to the simple structure of the function $\chi(\alpha, R)$, which is singular only at one point $\alpha=0$ and does not depend on θ because of the s -wave boundary condition. Following Eq. (7), the boundary condition for the function $\chi(\alpha_i, R)$ takes the form

$$\lim_{\alpha_i \rightarrow 0} \left[\frac{\partial \chi(\alpha_i, R)}{\partial \alpha_i} - \frac{1}{\alpha_i(R + \ln \alpha_i)} \sum_{j=1}^3 \chi(\alpha_j, R) \right] = 0, \quad (16)$$

where the sum contains two functions $\chi(\alpha_j, R)$ (for $j \neq i$), which are regular in the limit $\alpha_i \rightarrow 0$. The solution to the eigenvalue problem on the hypersphere is straightforward in terms of the Legendre function $P_\nu(x)$ regular at $x=1$ [52],

$$\chi(\alpha, R) = A(R) P_{[\xi(R)-1]/2}(-\cos 2\alpha), \quad (17)$$

where $A(R)$ is the normalization constant. Substituting Eq. (17) into the boundary condition (16), using the asymptotic form of the Legendre function as $\alpha \rightarrow 0$, $P_\nu(-\cos 2\alpha)$

$\rightarrow \frac{2}{\pi} \sin \pi \nu [\ln \alpha + \gamma + \psi(\nu+1)] + \cos \pi \nu$ [52], and calculating the limit $\cos 2\alpha_{j,k} \rightarrow -1/2$ as $\alpha_i \rightarrow 0$, one comes to the eigenvalue equation

$$R - \gamma - \psi\left(\frac{\xi+1}{2}\right) + \frac{\pi}{2} \tan \frac{\pi}{2} \xi + \pi \sec \frac{\pi}{2} \xi P_{(\xi-1)/2}\left(\frac{1}{2}\right) = 0, \quad (18)$$

where $\psi(x)$ is the digamma function. The same eigenvalue equation, in slightly different notation, was derived in Ref. [44] in the limit of the zero interaction range.

Considering the solution of Eq. (18), it is worthwhile to note that the left-hand side is an even function of ξ ; i.e., R is a function of ξ^2 . Similar to the corresponding eigenvalue equation in 3D [34,35], the transcendental equation (18) determines the infinitely multivalued function $\xi^2(R)$ for an arbitrary complex-valued variable R . In particular, different branches of this unique function for the real-valued R form a set of real-valued $\xi_n^2(R)$ which play the role of eigenpotentials in the HRE's. Hereafter it is convenient to enumerate $\xi_n^2(R)$ by an index $n=1, 2, 3, \dots$ in ascending order. As R increases from $-\infty$ to ∞ , all the terms $\xi_n^2(R)$ decrease monotonically in the intervals $-\infty < \xi_1^2(R) < 1$, $1 < \xi_2^2(R) < 25$, and $(2n-1)^2 < \xi_n^2(R) < (2n+1)^2$ for $n > 2$. Note that at the exceptional point $\xi=3$ the solution of the eigenvalue equation (18) gives a finite limit $R_0 \approx 1.64$; nevertheless, calculation of the function $\xi_2^2(R)$ and its derivatives in the vicinity of this point requires special care to take into account exact cancellation of divergent terms.

B. Derivation of the coupling terms

An important advantage of the BCM is the analytical expression (18) for the eigenpotentials $\xi_n^2(R)$ in HRE's that allows one to study the asymptotic properties of the solution and to simplify the numerical calculation thus improving its accuracy. Evidently, the analytical expressions are strongly desirable for the coupling terms $Q_{nm}(R)$ and $P_{nm}(R)$. Whereas direct evaluation of $Q_{nm}(R)$ and $P_{nm}(R)$ by means of the definitions (12) and (13) is quite involved, fortunately one can circumvent this obstacle by using the explicit dependence on the parameter R in the eigenvalue problem (6) and (7). Thus, within the framework of the BCM one derives the analytical expression for $Q(\rho)$ and $P(\rho)$ via eigenpotentials $\xi_n^2(R)$ and their derivatives over R .

To simplify the notation, the eigenvalue problem of the hypersphere (6) and (7) is written as

$$(\Lambda^2 - \varepsilon_n)\Phi_n = 0, \quad (19)$$

$$\lim_{\alpha_i \rightarrow 0} \left(\frac{\partial \Phi_n}{\partial \alpha_i} - \frac{\phi_n}{\alpha_i} \right) = 0, \quad (20)$$

where $\varepsilon_n = -\xi_n^2 + 1$ and the function

$$\phi_n(\alpha, R) = \frac{\Phi_n(\alpha, R)}{\ln \alpha + R} \quad (21)$$

tends, as $\alpha \rightarrow 0$, to a finite limit which does not depend on the index enumerating the different sets of the Jacobi coor-

dinates. Taking the derivatives of Eqs. (19) and (20) with respect to R , one obtains that Φ'_n satisfy the inhomogeneous equation

$$(\Lambda^2 - \varepsilon_n)\Phi'_n = \varepsilon'_n \Phi_n \quad (22)$$

and the boundary condition

$$\lim_{\alpha_i \rightarrow 0} \left(\frac{\partial \Phi'_n}{\partial \alpha_i} - \frac{\phi'_n}{\alpha_i} \right) = 0. \quad (23)$$

For derivation of $Q_{nm}(R)$, one starts with the Hellmann-Feynman-type relation

$$\langle \Phi_m | \Lambda^2 | \Phi'_n \rangle - \langle \Phi'_n | \Lambda^2 | \Phi_m \rangle = \varepsilon'_n \delta_{nm} + (\varepsilon_m - \varepsilon_n) Q_{nm}, \quad (24)$$

which is obtained by projecting Eqs. (19) and (22) onto the functions Φ'_m and Φ_m , respectively. On the other hand, the integrals over the hypersphere on the left-hand side of Eq. (24) reduce to contour integrals around three points $\alpha_i=0$ in which the functions Φ_n and Φ'_n have singularities. Allowing the length of the contours to shrink to zero and taking into account that all three singular points $\alpha_i=0$ make equal contributions for the symmetry reason, one obtains

$$\langle \Phi_m | \Lambda^2 | \Phi'_n \rangle - \langle \Phi'_n | \Lambda^2 | \Phi_m \rangle = \lim_{\alpha \rightarrow 0} \alpha \left[\Phi'_n \frac{\partial \Phi_m}{\partial \alpha} - \Phi_m \frac{\partial \Phi'_n}{\partial \alpha} \right]. \quad (25)$$

Combining the boundary conditions (20) and (23) with Eq. (21), one finds

$$\lim_{\alpha \rightarrow 0} \alpha \left[\Phi_m \frac{\partial \Phi'_n}{\partial \alpha} - \Phi'_n \frac{\partial \Phi_m}{\partial \alpha} \right] = \phi_n(0, R) \phi'_m(0, R), \quad (26)$$

which eventually leads to the basic relation

$$\varepsilon'_n \delta_{nm} + (\varepsilon_m - \varepsilon_n) Q_{nm} - \phi_n(0, R) \phi'_m(0, R) = 0. \quad (27)$$

The diagonal part of Eq. (27) provides a simple relation between $\phi_n(0, R)$ and ε'_n ,

$$\varepsilon'_n - \phi_n^2(0, R) = 0, \quad (28)$$

while the nondiagonal part of Eq. (27) combined with Eq. (28) gives finally the desired result

$$Q_{nm} = \frac{\sqrt{\varepsilon'_n \varepsilon'_m}}{\varepsilon_m - \varepsilon_n}. \quad (29)$$

In a similar way, to derive $P_{nm}(R)$ for $n \neq m$, one calculates the difference $\langle \Phi'_m | \Lambda^2 | \Phi'_n \rangle - \langle \Phi'_n | \Lambda^2 | \Phi'_m \rangle$ by projecting Eq. (22) onto the functions $\Phi'_{n,m}$ and integrating on the hypersphere, which gives

$$(\varepsilon_n - \varepsilon_m) P_{nm} + (\varepsilon'_n + \varepsilon'_m) Q_{nm} = - \lim_{\alpha \rightarrow 0} \alpha \left[\Phi'_m \frac{\partial \Phi'_n}{\partial \alpha} - \Phi'_n \frac{\partial \Phi'_m}{\partial \alpha} \right]. \quad (30)$$

In view of Eqs. (20) and (23), the limit on the right-hand side of Eq. (30) equals $\phi'_m(0, R) \phi'_n(0, R) - \phi_n(0, R) \phi'_m(0, R)$, which allows one to obtain, by expressing $\phi_n(0, R)$, $\phi'_n(0, R)$ via ε'_n , ε'_n from Eq. (28),

$$P_{nm} = Q_{nm} \left[\frac{\varepsilon'_n + \varepsilon'_m}{\varepsilon_m - \varepsilon_n} + \frac{1}{2} \left(\frac{\varepsilon''_n}{\varepsilon'_n} - \frac{\varepsilon''_m}{\varepsilon'_m} \right) \right]. \quad (31)$$

For derivation of the diagonal terms $P_{nn}(R)$, one requires functions Φ'_n , which satisfy the inhomogeneous equation

$$(\Lambda^2 - \varepsilon_n)\Phi''_n = 2\varepsilon'_n \Phi'_n + \varepsilon''_n \Phi_n \quad (32)$$

and the boundary condition

$$\lim_{\alpha_i \rightarrow 0} \left(\frac{\partial \Phi''_n}{\partial \alpha_i} - \frac{\phi''_n}{\alpha_i} \right) = 0. \quad (33)$$

Repeating the above procedure to calculate the difference $\langle \Phi'_n | \Lambda^2 | \Phi''_n \rangle - \langle \Phi''_n | \Lambda^2 | \Phi'_n \rangle$ and taking into account the identity $P_{nn} = -\langle \Phi''_n | \Phi_n \rangle$ one obtains

$$\begin{aligned} 3\varepsilon'_n P_{nn} &= \lim_{\alpha \rightarrow 0} \alpha \left[\Phi'_n \frac{\partial \Phi''_n}{\partial \alpha} - \Phi''_n \frac{\partial \Phi'_n}{\partial \alpha} \right] \\ &= 2[\phi'_n(0, R)]^2 - \phi_n(0, R) \phi''_n(0, R), \end{aligned} \quad (34)$$

which after simple algebra in combination with Eq. (28) gives rise to

$$P_{nn} = -\frac{1}{6} \frac{\varepsilon'''_n}{\varepsilon'_n} + \frac{1}{4} \left(\frac{\varepsilon''_n}{\varepsilon'_n} \right)^2. \quad (35)$$

The derivation of all the terms in HRE's is accomplished with the exact expressions (29), (31), and (35) for the coupling terms $Q_{nm}(R)$ and $P_{nm}(R)$ and the eigenvalue equation (18) for $\xi^2(R)$. Whereas the explicit value of $\phi_n(0, R)$ is of no interest for determination of $Q_{nm}(R)$ and $P_{nm}(R)$, it is easy to calculate the limit $\alpha \rightarrow 0$ in Eq. (21),

$$\phi_n(0, R) = \frac{2}{\pi} A_n \cos \frac{\pi}{2} \xi_n, \quad (36)$$

which, in view of Eq. (28), allows the normalization constant to be additionally determined,

$$A_n = \frac{\pi}{2} \sqrt{-2\xi_n \varepsilon'_n} \sec \frac{\pi}{2} \xi_n. \quad (37)$$

One should emphasize the generality of the derived analytical expressions (29), (31), and (35). The derivation is based essentially on the BCM used to describe the pairwise interaction. Within the framework of the BCM the described procedure is applicable to the derivation of the coupling terms for a variety of three-body systems in the configuration space of an arbitrary dimension including particles of different masses and scattering lengths and particles with internal degrees of freedom. In particular, analytical expressions of the same form are valid for three identical bosons in 3D [35] and 1D (discussed in the Appendix) and for three two-species fermions in 3D [53].

C. Asymptotic expansions and boundary conditions for HRE's

Asymptotic expansions for all the terms of HRE's are of interest for a qualitative study of the described three-body system. In addition, the explicit asymptotic form allows one

to formulate the boundary conditions and to improve the accuracy of the numerical calculations. The analytical expressions derived in the preceding sections provide a straightforward determination of the eigenpotentials and the coupling terms in the asymptotic region $|R| \rightarrow \infty$.

The expansion of eigenpotentials $\xi_n^2(R)$ at $|R| \rightarrow \infty$ follows from the expansion of the eigenvalue equation (18) at the singular points—i.e., near the odd integer ξ (except $\xi=3$) and at infinite ξ . In particular, the expansion at $\xi \rightarrow i\infty$ provides the lowest eigenpotential at $R \rightarrow \infty$

$$\xi_1^2(R) = -4e^{2(R-\gamma)} - \frac{1}{3} - \frac{2}{45}e^{-2(R-\gamma)} + O(e^{-4R}). \quad (38)$$

The neighboring branches of the multivalued function $\xi(R)$ are continuously connected at infinity so that $\xi_n(R)$ at $R \rightarrow \infty$ is continuation of $\xi_{n-1}(R)$ at $R \rightarrow -\infty$. Thus, the same asymptotic expansion at $R \rightarrow \infty$ for $\xi_n(R)$ and $\xi_{n-1}(-R)$ is obtained by using the expansion of $R(\xi)$ near the odd integer ξ ,

$$\xi_n(R) = \xi_{n-1}(-R) = \begin{cases} 1 + \frac{3}{R + \ln(4/3)} + O(|R|^{-3}), & n = 2, \\ 2n - 1 + \frac{1 - 2(-1)^n P_{n-1}(1/2)}{R - \gamma - \psi(n) + (-1)^n \left. \frac{dP_\nu(1/2)}{d\nu} \right|_{\nu=n-1}} + O(|R|^{-3}), & n > 2. \end{cases} \quad (39)$$

As $\xi_n(R)$ ($n \geq 2$) are of the smoothed-step form with the steepest descent at $R \approx \ln n$, the asymptotic expansion (39) is not uniform in n —viz., it is valid only if $R \gg \ln n$ —which hinders any consideration of the infinite- n limit. Therefore, one needs the asymptotic expansion at $R \rightarrow \infty$ which reproduces the steplike dependence of $\xi_n(R)$ at least in the large- n limit, thus being applicable for both large R and n . The expansion is constructed by using the requirement that both the $\xi_n(R)$ and their derivatives over R for $n > 2$ coincide with the exact result at the point $\bar{R}_n = \gamma + \psi(n+1/2) - (-1)^n \pi P_{n-1/2}(1/2)$ —viz., one requires $\xi_n(\bar{R}_n) = 2n$ and $\xi'_n(\bar{R}_n) = -4 \left[\pi^2 - 2\psi'(n+1/2) + (-1)^n 2\pi \left. \frac{\partial P_\nu(1/2)}{\partial \nu} \right|_{\nu=n-1/2} \right]^{-1}$ —which leads to the result

$$\xi_n(R) \approx 2n + \frac{2}{\pi} \left[\arctan x_n + (-1)^n \arcsin \frac{\pi \xi'_n(\bar{R}_n) P_{n-1/2}(1/2)}{\sqrt{x_n^2 + 1}} \right], \quad (40)$$

where $x_n = \frac{\pi}{2} \xi'_n(\bar{R}_n) [R - \gamma - \psi(n+1/2)]$. As follows from Eq. (40), $\xi_n(R)$ (properly shifted along both coordinate axes) at large n converge to the function $\xi_n(R) \approx 2n - \frac{2}{\pi} \arctan \frac{2}{\pi} (R - \ln n - \gamma)$. The quite slow (as $n^{-1/2}$) large- n convergence is entirely determined by the asymptotic behavior of the Legendre function as $\nu \rightarrow \infty$, $P_{\nu-1/2}(1/2) \sim \nu^{-1/2} \cos \pi(\nu/3 - 1/4)$ [52]. Actually, the terms of order $\sim n^{-1/2}$ contain the dependence on n via the expressions $(-1)^n \cos \pi(n/3 - 1/4)$ and $(-1)^n \sin \pi(n/3 - 1/4)$, which are periodic functions of n with period 3. Thus, one concludes that $\xi_n(R)$ up to leading-order terms in n belong to three families for different $n \bmod 3$. Convergence to the unique function is illustrated in Fig. 1 for two families of $\xi_n(R)$.

Substituting the above expansions for $\xi_n(R)$ in the analytical expressions derived in Sec. III B, one obtains asymptotic expansions of the coupling terms. A separate expression for the first-channel diagonal coupling term at $R \rightarrow \infty$ follows from Eq. (38),

$$P_{11}(R) = 1/3 + 2/45 e^{-4(R-\gamma)} + O(e^{-6R}). \quad (41)$$

Furthermore, using the expansions (39) one finds that $Q_{nm}(R)$ decrease as $|R|^{-2}$ and $P_{nm}(R)$ decrease as $|R|^{-4}$ except the terms $Q_{n1}(R)$ and $P_{n1}(R)$ at positive R , which decrease as $Q_{n1}(R) \sim P_{n1}(R) \sim e^{-R} R^{-1}$ at $R \rightarrow \infty$ provided $R \gg \ln n$. As discussed above, this asymptotic dependence is not uniform in n and one would use the expression (40) to obtain the uniform expansion which is valid for large n . For example, the desired expansion for $Q_{nm}(R)$ at $R \rightarrow \infty$ takes the form

$$Q_{n1}(R) \approx \frac{\pi \xi'_n(\bar{R}_n)}{4n} \left[\frac{\xi_n(R)}{x_n^2 + 1} \left(1 - \frac{(-1)^n 2x_n P_{n-1/2}(1/2)}{\sqrt{x_n^2 + 1}} \right) \right]^{1/2} \times \left[\cosh \left(\frac{2x_n}{\pi \xi'_n(\bar{R}_n)} \right) \right]^{-1}. \quad (42)$$

Similar to $\xi_n(R)$, both $Q_{nm}(R)$ and $P_{nm}(R)$ (properly scaled and shifted along the coordinate axis) converge at large n to the universal limiting functions so that $Q_{n1}(R) \rightarrow (2n)^{-1/2} \tilde{Q}_1(R - \ln n - \gamma)$, $P_{n1}(R) \rightarrow (2n)^{-1/2} \tilde{P}_1(R - \ln n - \gamma)$, $P_{nm}(R) \rightarrow \tilde{P}(R - \ln n - \gamma)$, and $Q_{nm}(R) \rightarrow \tilde{Q}(n/m, R - \ln n - \gamma)$ for $n > m$, where

$$\tilde{Q}_1(y) = (y^2 + \pi^2/4)^{-1/2} (\cosh y)^{-1}, \quad (43)$$

$$\tilde{P}_1(y) = \tilde{Q}_1(y) \left(\tanh y - \frac{y}{y^2 + \pi^2/4} \right), \quad (44)$$

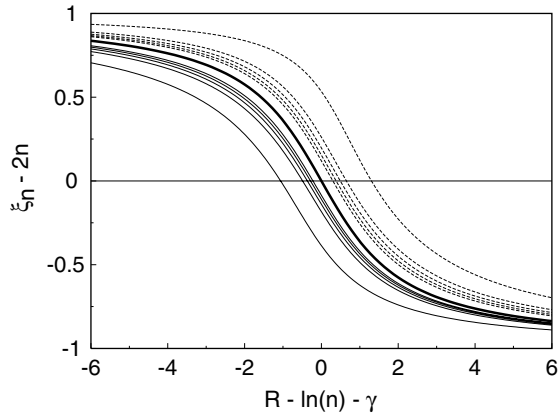


FIG. 1. Convergence of eigenvalues $\xi_n(R)$ to the limiting function (bold line). Two families of $\xi_n(R)$ are plotted by solid lines for $n=3m$ and by dashed lines for $n=3m+1$, $m=1, 5, 9, 15, 25$.

$$\tilde{P}(y) = \frac{\pi^2}{12(y^2 + \pi^2/4)^2}, \quad (45)$$

$$\tilde{Q}(z, y) = z^{1/2} \{(z^2 - 1)(y^2 + \pi^2/4)[(y + \ln z)^2 + \pi^2/4]\}^{-1/2}. \quad (46)$$

Splitting of eigenpotentials into three families depending on $n \bmod 3$ entails a corresponding splitting of the coupling terms. The splitting and convergence to the universal limiting functions for $Q_{n1}(R)$ and $P_{n1}(R)$ are illustrated in Fig. 2.

At infinite separation of particles—i.e., when $R \rightarrow \infty$ —the leading term of the asymptotic expansion for the first eigenpotential is related to the dimensionless energy of the two-body bound state so that $\xi_1^2 e^{-2R} = \xi_1^2 / \rho^2 \rightarrow -4e^{-2\gamma} \approx -1.261$, while for other eigenpotentials the leading terms in the upper channels are related to the kinematic barriers, $\xi_2^2 e^{-2R} \rightarrow 1/\rho^2$ and $\xi_n^2 e^{-2R} \rightarrow (2n-1)^2/\rho^2$ for $n > 2$. Thus, in the asymptotic region, the first-channel component of the total wave function describes the two-cluster $2+1$ configuration, whereas the upper-channel components describe the three-cluster configuration.

Using the expansion of $\xi_1(R)$ at $R \rightarrow -\infty$, Eq. (39), one obtains the asymptotic form of the first-channel radial function at a small hyperradius:

$$f_1(R) \sim e^R \left(R + \ln \frac{4}{3} \right)^2 \left(R + \ln \frac{4}{3} - \frac{3}{2} \right). \quad (47)$$

Given the expansion of $\xi_1(R)$, Eqs. (15), (17), and (37), and the expansion of the Legendre function at $\nu \rightarrow 0$, $P_\nu(-\cos 2\alpha) \approx 1 + 2\nu \ln \sin \alpha$ [52], the asymptotic form of the first eigenfunction on the hypersphere at $R \rightarrow -\infty$ is

$$\Phi_1(\alpha, R) \sim \left(R + \ln \frac{4}{3} \right)^{-2} \left(R + \ln \frac{4}{3} + \frac{3}{2} \right) \left(R + \ln \frac{4}{3} + \sum_i \ln \sin \alpha_i \right). \quad (48)$$

As the first-channel contribution dominates in the series (5), the expressions (47) and (48) entail the asymptotic form of

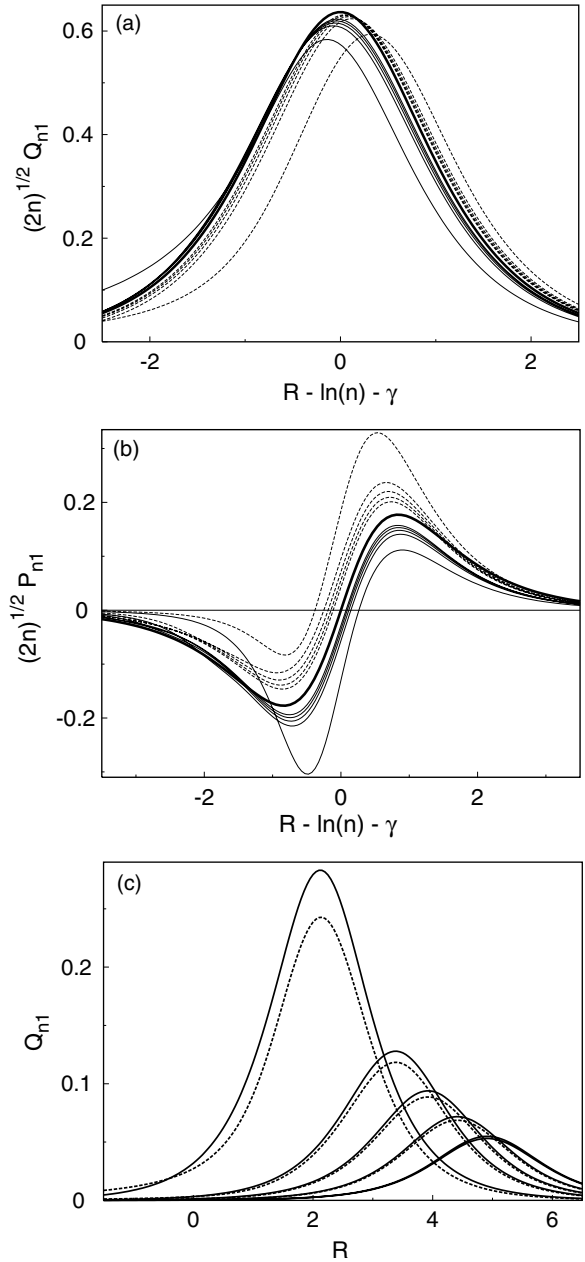


FIG. 2. Two families of $Q_{n1}(R)$ (a) and $P_{n1}(R)$ (b) are plotted by solid lines for $n=3m$ and by dashed lines for $n=3m+1$, $m=1, 5, 9, 15, 25$. The corresponding limiting functions $\tilde{Q}_1(R - \ln n - \gamma)$ and $\tilde{P}_1(R - \ln n - \gamma)$ are plotted by a bold line. In panel (c) the exact result (solid lines) and the asymptotic expression (42) (dashed lines) are compared for the third family of $Q_{n1}(R)$ ($n=3m+2$, $m=1, 5, 9, 15, 25$).

the total wave function at $R \rightarrow -\infty$ —i.e., near the triple-collision point,

$$\begin{aligned} \Psi &\sim \left(R + \ln \frac{4}{3} \right)^2 \left(\sum_i \ln \sin \alpha_i + R + \ln \frac{4}{3} \right) \\ &= \ln^2 \frac{4}{3} \rho \ln \frac{4x_1 x_2 x_3}{3\rho^2}. \end{aligned} \quad (49)$$

In addition, the nonsingularity of the lowest eigenpotential in

the limit of a small hyperradius $R \rightarrow -\infty$ leads to the well-known conclusion that neither the Efimov nor Thomas effect exists in 2D [8,9,23].

For the eigenvalue problem—i.e., for calculation of the bound-state energies—the solutions satisfy the requirement of the square integrability of the total wave function, $\sum_n \int_{-\infty}^{\infty} f_n^2(R) e^{2R} dR = 1$, and in practice one can use boundary conditions for the channel functions of the form $f_n(R) \rightarrow 0$ at $R \rightarrow \pm\infty$. For 2+1 scattering below the three-body threshold, the wave function in the asymptotic region tends to a product of the two-body bound-state wave function $\varphi(x)$ and the function $F(r)$, which depends on the intercluster distance $r = \sqrt{3}y/2$ and describes relative motion of two clusters. The (2+1)-scattering length A enters in the asymptotic expression for $F(r)$ at the zero kinetic energy of two colliding clusters, $F(r) \sim \ln(r/A)$, which corresponds to the asymptotic form of the total wave function, $\Psi(\mathbf{x}, \mathbf{y}) \rightarrow \varphi(x) \ln \frac{\sqrt{3}y}{2A}$ as $y \rightarrow \infty$. Taking into account that the first-channel eigenfunction $\Phi_1(\alpha, \theta, R)$ at a large hyperradius reduces to $\varphi(x)e^R$ and $y \approx \rho = e^R$ for $x \ll y$, one finds the asymptotic form of the channel function $f_1(R)$,

$$f_1(R) \sim \ln \frac{2A}{\sqrt{3}} - R, \quad R \rightarrow \infty. \quad (50)$$

In addition to the asymptotic expression (50) at $R \rightarrow \infty$, the first-channel function $f_1(R) \rightarrow 0$ at $R \rightarrow -\infty$, while all other channel functions $f_n(R) \rightarrow 0$, $n \geq 2$, at both limits $R \rightarrow \pm\infty$.

The asymptotic form of $\xi_1^2(R)$ and $P_{11}(R)$ at $R \rightarrow \infty$ are of fundamental importance in the analysis of the low-energy 2+1 scattering. In the lowest channel of HRE's, the leading term of $\xi_1^2(R)$, Eq. (38), cancels the term Ee^{2R} for the threshold energy $E = -4e^{-2\gamma}$ and the next-order constant $1/3$ terms of $\xi_1^2(R)$, Eq. (38), and $P_{11}(R)$, Eq. (41), cancel each other; therefore, the effective interaction takes the form $\frac{2}{45}e^{-2(R-\gamma)}$, which corresponds to the polarization interaction $V_p = -\alpha/(2r^4)$, where r is the distance between a dimer and the third particle and $\alpha = e^{2\gamma}/20 \approx 0.1586$. This long-range polarization tail of the effective interaction is a specific 2D feature (compare, e.g., the exponential falloff of the lowest effective interaction at large distances for three bosons in 3D [35]). The (2+1)-scattering length in 2D exists even if the effective interaction contains the polarization tail [48,49] (in fact, for the potentials decreasing faster than $1/\rho^{2+\delta}$). This can be seen from the asymptotic solution of the first-channel HRE of the system (9) at the threshold energy, $E = -4e^{-2\gamma}$. Up to terms of order $O(e^{-2R})$, the first-channel HRE takes the form

$$\left[\frac{d^2}{dR^2} + \frac{2}{45}e^{-2(R-\gamma)} \right] f_1(R) = 0. \quad (51)$$

The general solution of Eq. (51) is the linear combination of the Bessel functions

$$f_1(R) \sim C_1 J_0(\sqrt{2/45}e^{-R+\gamma}) + C_2 Y_0(\sqrt{2/45}e^{-R+\gamma}). \quad (52)$$

The asymptotic expansion of the solution (52) at $R \rightarrow \infty$, $f_1(R) \sim \frac{\pi C_1}{2C_2} + 2\gamma - \frac{1}{2} \ln 90 - R$, is of the form (50), which proves the existence of the scattering length A . As a consequence, the leading-order terms of the effective-range expansion

for 2+1 scattering are of the usual form (1) for two-body scattering in 2D—viz., $\frac{\pi}{2} \cot \delta(k) \approx \ln(kA/2) + \gamma$, where k is the wave number for the relative motion of a dimer and the third particle. Nevertheless, the higher terms of the effective-range expansion are modified by the polarization tail of the effective interaction as is known to be the case in 3D scattering [54].

The role of the long-range term $\sim e^{-2R}$ or $\sim \rho^{-4}$ in the first-channel HRE requires a careful treatment because there is no clear reason for appearance of the polarization potential between a particle and a bound pair. In this respect, it is necessary to study a contribution of the upper channels to the effective dimer-particle interactions at long distances. Coupling with the upper channels produces in the first channel the nonlocal effective potential $U_c(R, R')$ which can be estimated in the lowest order of perturbation theory as $U_c(R, R') = \sum_n^\infty F_n(R) g_n(R-R') F_n(R')$, where $F_n(R) = Q_{n1}(R) \frac{d}{dR} + \frac{d}{dR} Q_{n1}(R) + P_{n1}(R)$ and $g_n(R-R')$ is Green's function in the n th channel. Taking into account that $\xi_n^2(R) \sim 4n^2$, $Q_{n1}(R) = (2n)^{-1/2} \tilde{Q}_1(R - \ln n - \gamma)$, and $P_{n1}(R) = (2n)^{-1/2} \tilde{P}_1(R - \ln n - \gamma)$ for large n , one can estimate $g_n(x) \sim (4n)^{-1} e^{-2n|x|}$ and $F_n(R) \sim n^{-1/2} \tilde{F}(R - \ln n)$, where $\tilde{F}(x)$ is expressed via $\tilde{Q}_1(x)$ and $\tilde{P}_1(x)$. As $g_n(x) \rightarrow (2n)^{-2} \delta(x)$ for $n \rightarrow \infty$, these estimates entail the following local limit of $U_c(R, R')$: viz., $U_c(R) \sim \sum_n^\infty n^{-3} \tilde{F}^2(R - \ln n)$. Summing over n , one finds that the leading term of the effective potential is $U_c(R) \sim e^{-2R}$; in other words, coupling with the upper channels produces in the first channel the long-range term of the same order $\sim e^{-2R}$ or $\sim \rho^{-4}$ as the above-discussed polarization tail. Thus, any conclusion on the long-range behavior of the wave function or, equivalently, on the next-to-leading terms of the effective-range expansion for 2+1 scattering must be based on the study of a large number of HRE's.

IV. NUMERICAL CALCULATIONS

The eigenpotentials $\xi_n^2(R)$ and the coupling terms $P_{nm}(R)$ and $Q_{nm}(R)$ in HRE's were calculated by solving the transcendental eigenvalue equation (18) and by using Eqs. (29), (31), and (35). The derivatives with respect to R (ξ_n' , ξ_n'' , and ξ_n''') were replaced by the derivatives of the inverse function ($dR/d\xi$, $d^2R/d\xi^2$, and $d^3R/d\xi^3$) which are easily calculable from the eigenvalue equation (18). The most involved numerical problem is to calculate the Legendre function and its derivatives with respect to the index entering into Eqs. (18), (29), (31), and (35). This is done for both real and imaginary ξ by using the Mehler-Dirichlet integral representation [52]

$$P_{(\xi-1)/2} \left(\frac{1}{2} \right) = \frac{\sqrt{2}}{\pi} \int_0^{\pi/3} \frac{dt \cos \frac{\xi}{2} t}{\sqrt{\cos t - 1/2}} \quad (53)$$

for the Legendre function and using for its derivatives the corresponding integral representations obtained by differentiating Eq. (53) with respect to ξ . The terms containing an integrable square-root singularity are subtracted from the integrand and calculated exactly to improve the accuracy. As a

result, the Legendre function was calculated with a relative accuracy about 10^{-11} whereas the accuracy degraded about one order for each of the subsequent derivatives. As mentioned in Sec. III C, accuracy of the numerical calculation suffers from the subtraction of divergent terms in the vicinity of the exceptional point $\xi=3$. For this reason, $\xi_2(R)$, $Q_{2n}(R)$, and $P_{2n}(R)$ in a narrow region around the point $R_0 \approx 1.64$ [which corresponds to $\xi_2(R_0)=3$] were obtained by the interpolation procedure. Under the described approximations, the overall relative accuracy was not worse than 10^{-11} for the eigenpotentials and 10^{-8} for the coupling terms. It is worthwhile to mention that a less accurate calculation of the coupling terms is in accordance with a smaller contribution of these terms to the final values. The sum rule (14) for the coupling terms was numerically checked, and it was found that the difference $\sum_{k=1}^N Q_{nk}Q_{mk} - P_{nm}$ decreases as N^{-2} with increasing N . The eigenpotentials and all the coupling terms for the four lowest channels of HRE's are shown in Figs. 3 and 4.

For a numerical solution, the truncated system of N HRE's is reduced to the form without the first derivatives by the transformation $\mathbf{f}(R) = \mathbf{T}(R)\tilde{\mathbf{f}}(R)$, where the orthogonal matrix $\mathbf{T}(R)$ satisfies the equation

$$\frac{d\mathbf{T}}{dR} + \mathbf{Q}\mathbf{T} = 0. \quad (54)$$

Furthermore, one introduces the antisymmetric matrix \mathbf{B} by the Cayley transform, $\mathbf{B} = (\mathbf{T}-1)(\mathbf{T}+1)^{-1}$, and solves the equation

$$2\frac{d\mathbf{B}}{dR} = (\mathbf{B}-1)\mathbf{Q}(\mathbf{B}+1). \quad (55)$$

This form is preferable because one can use only the upper triangle of the matrices \mathbf{B} and \mathbf{Q} in the numerical calculations, which gives the antisymmetric matrix \mathbf{B} and the orthogonal matrix $\mathbf{T} = (1-\mathbf{B})(1+\mathbf{B})^{-1}$ independently of the round-off error. Note that in the two-channel approximation the nonzero matrix elements of \mathbf{B} are explicitly expressed via the quadrature, $B_{21} = -B_{12} = \tan \frac{1}{2} \int Q_{12}(R) dR$.

Following the described procedure, the truncated system of N HRE's in two forms (9) and (10) was numerically solved on the finite interval $[R_{min}, R_{max}]$. At the first step, Eq. (55) was integrated and the matrix $\mathbf{T} = (1-\mathbf{B})^{-1}(1+\mathbf{B})$ was determined at the mesh points on $[R_{min}, R_{max}]$. An arbitrary antisymmetric matrix \mathbf{B}_0 serves as the initial condition for the matrix equation (55) imposed at R_{min} . The consistency of the numerical procedure was additionally shown by checking the stability of the calculated values for different choices of the initial matrix $\mathbf{T}(R_{min})$. Given the calculated transformation matrix $\mathbf{T}(R)$, two eigenenergies and the scattering length were calculated by solving the eigenvalue problem and the scattering problem at the threshold energy $E = -4e^{-2\gamma}$ for the transformed HRE's. The zero-boundary conditions are imposed in the upper channels—i.e., $f_n(R_{min}) = f_n(R_{max}) = 0$ for $n \geq 2$ —whereas the left-end boundary condition in the first channel was determined from the asymptotic form of the $f_1(R)$ at $R \rightarrow -\infty$, Eq. (47). At the right boundary, one uses

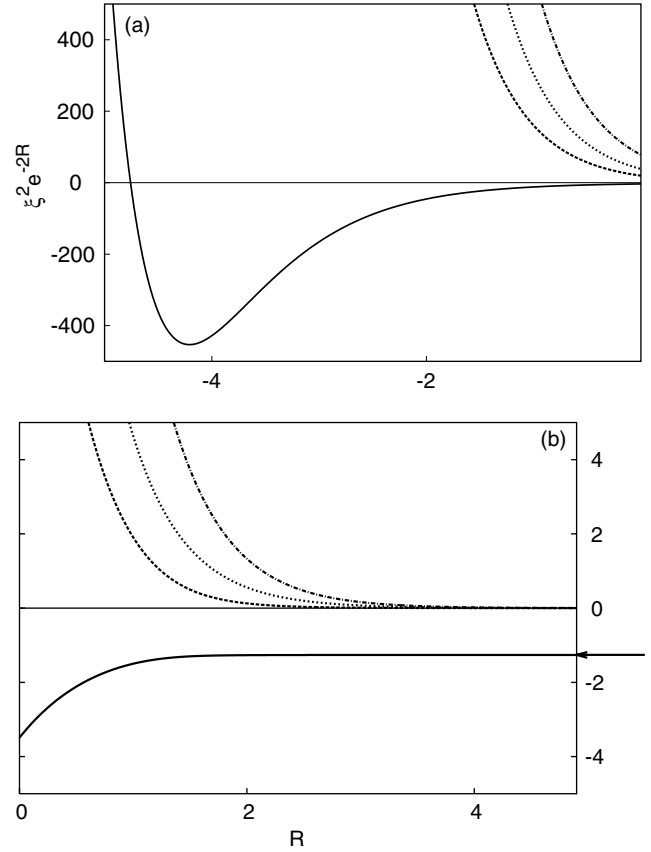


FIG. 3. The lowest scaled eigenpotentials $\xi_n^2(R)e^{-2R}$. Notice different scales for the positive and negative R . The arrow marks the two-body bound-state energy $-4e^{-2\gamma}$.

$f_1(R_{max}) = 0$ for the eigenvalue problem and the asymptotic form (52) for the scattering problem. In the latter case, the scattering length is determined via the coefficients $C_{1,2}$ calculated at R_{max} —viz., $\ln A = \frac{\pi}{2} \frac{C_1}{C_2} + 2\gamma - \frac{1}{2} \ln 120$ —thus taking into account the polarization tail of the effective interaction beyond the integration region. The boundary conditions for the vector function $\tilde{\mathbf{f}}(R)$ were obtained by applying the transformation $T(R)$ at the points R_{min} and R_{max} .

The overall accuracy of the numerical procedure is estimated to provide the calculation of the binding energies and the scattering length with the relative error about 3×10^{-8} and 1×10^{-6} , respectively. In particular, a sufficient accuracy of numerical integration of HRE's was obtained by taking $R_{min} = -14$ and $R_{max} = 1.5, 3.5,$ and 6.0 for the ground-state, the excited-state, and the scattering-length calculations, respectively. The structure of the calculated wave function is illustrated in Fig. 5, where the four lowest channel functions $f_n(R)$ for the ground state, excited state, and the scattering state are shown. For convenience, the solution of the scattering problem is normalized to match the first-channel functions of the excited and scattering states at the point $R \approx -3.1$ corresponding to the first maximum. The numerical solution of the truncated system of N HRE's provides a set of binding energies and scattering lengths, which are presented in Table I in comparison with the calculations [8,29,44]. It is clearly seen that highly accurate results can be obtained by

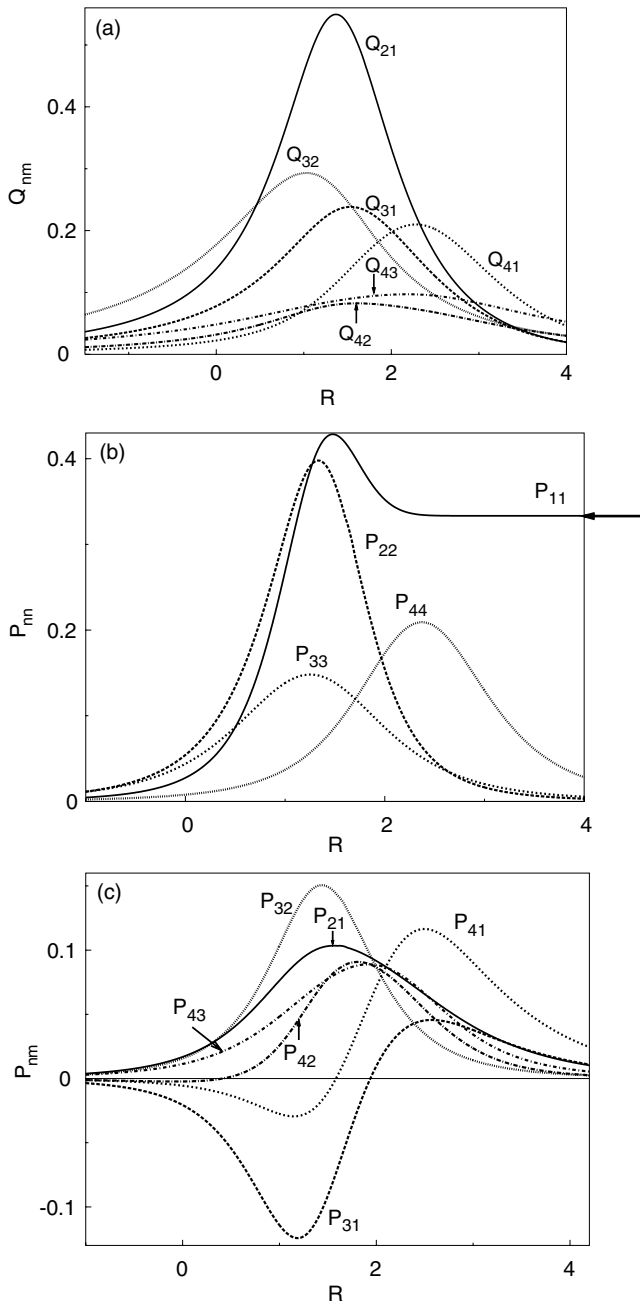


FIG. 4. Coupling terms $Q_{nm}(R)$ (a), $P_{nn}(R)$ (b), and $P_{nm}(R)$ for $n \neq m$ (c). The arrow marks the large hyperradius limit $1/3$ of $P_{11}(R)$.

means of the few-channel calculation of the form (9). The contribution to the binding energies from the upper channels (for $N \geq 16$) turns out to be comparable with the numerical accuracy. The role of the upper channels can be estimated by fitting to the simple power dependence on N , which is routinely used in the variational calculations. In the present calculations, it is reasonable to fit separately each of three families—i.e., to take into account the periodic dependence on N for $N=3m, 3m+1, 3m+2$. The calculated binding energies are fairly well fitted to the $a+b/N^c$ dependence for each family with the fitted value of power $c \approx 4$. The logarithm of the scattering length $\ln A$ converges slower than the binding

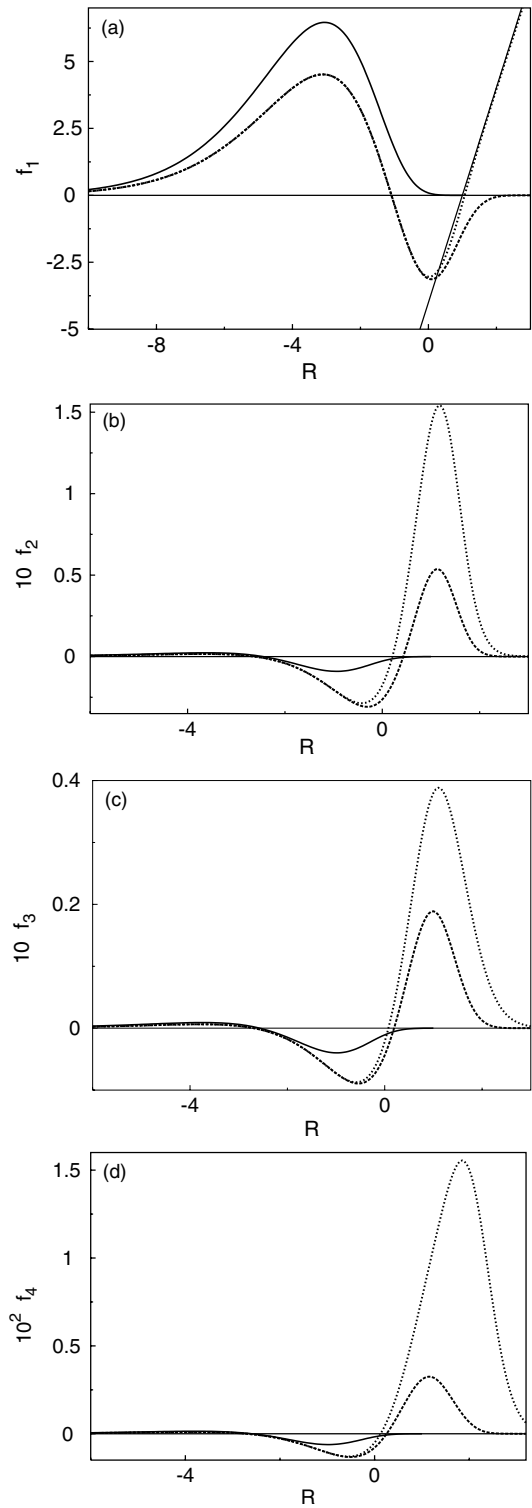


FIG. 5. Radial functions of the four lowest channels $f_1(R)$ (a), $f_2(R)$ (b), $f_3(R)$ (c), and $f_4(R)$ (d) for the ground state (solid lines), the excited state (dashed lines), and the scattering state calculated at the two-body threshold energy (dotted lines). For convenience, the radial functions for the excited state are multiplied by a factor of 5, while those for the scattering state are scaled to match at the first maximum the first-channel functions of the excited state and scattering state. Linear asymptotic dependence of the first-channel scattering solution is shown by a thin straight line in panel (a).

TABLE I. The three-body binding energies ε_0 and ε_1 (in units of the two-body binding energy) and the logarithm of the $(2+1)$ -scattering length A for identical bosons in 2D. The number of HRE's is denoted by N and the superscripts U and L mark the results obtained by solving HRE's of the form (9) and (10), respectively. Shown are also the results of fitting the dependence on N for the calculated binding energies and scattering length and those of other calculations.

N	ε_0^U	ε_0^L	ε_1^U	ε_1^L	$\ln A$
1	16.5194096	16.5788727	1.26667318	1.29214773	0.891305
2	16.5219444	16.5482471	1.26998847	1.27658964	0.858228
3	16.5226064	16.5302069	1.27033831	1.27263368	0.853238
4	16.5226348	16.5287316	1.27036317	1.27217992	0.851835
5	16.5226618	16.5267981	1.27039042	1.27147416	0.849801
6	16.5226787	16.5249848	1.27040205	1.27101864	0.848804
7	16.5226811	16.5246296	1.27040405	1.27091797	0.848343
8	16.5226835	16.5241930	1.27040625	1.27077981	0.847726
9	16.5226854	16.5237285	1.27040762	1.27066543	0.847341
10	16.5226859	16.5235979	1.27040796	1.27063093	0.847125
12	16.5226867	16.5232644	1.27040864	1.27054373	0.846651
14	16.5226870	16.5231314	1.27040883	1.27050912	0.846376
16	16.5226871	16.5230155	1.27040895	1.27048209	0.846186
∞	16.5226874		1.27040911		0.8451
Ref. [8]	16.1 \pm 0.2		1.25 \pm 0.05		
Ref. [44]	16.52		1.267		
Ref. [29]	16.522688		1.2704091		
Ref. [25]					≈ 1.1

energies, which is manifested by the smaller fitted power c within the range [1.0, 1.3]. The fitted binding energies and the scattering length corresponding to $N=\infty$ are presented in Table I with the overall fitting error in the last digit. As expected, the solution of the truncated system (10) provides slower convergence with increasing number of channels N than those of the form (9). The calculation based on the solution of the truncated system (10) gives a set of binding energies converging as N^{-2} , which is connected with the corresponding convergence rate of $\sum_{k=1}^N Q_{nk} Q_{mk}$ to P_{nm} .

The calculated binding energies coincide within the declared accuracy with the solution of the momentum-space integral equations [29], which underlines equivalence of quite different approaches. The binding energies of a limited accuracy obtained by solving the system of HRE's Ref. [44] are in agreement with the one-channel calculation of the present paper. The older results of [8] obtained by solving the integral equations are of low accuracy; in addition, the ground-state energy of [8] is above the upper bound found in the present paper. Calculations of the $(2+1)$ -scattering length are rarely available in the literature. The present calculation of the $(2+1)$ -scattering length in the universal limit could be compared with the results of Ref. [25] by analyzing the dependence of \bar{a}_3 on \bar{a}_2 shown in Fig. 1 of that paper. The three-boson scattering length \bar{a}_3 is related to the scattering length A defined in the present paper as $\bar{a}_3 = (2/\pi)\ln(2A/\sqrt{3})$, whereas the two-body scattering length \bar{a}_2 is defined in [25] so that the universal limit corresponds to $\bar{a}_2 \rightarrow 0$. Considering the smallest $\bar{a}_2 \approx 10^{-3}$ presented as the leftmost point in Fig. 1 of Ref. [25], one obtains

$\bar{a}_3 \approx 0.8$ —i.e., $\ln A \approx 1.1$ —which is well above the upper bound $\ln A \approx 0.8451$ calculated in the present paper. The discrepancy is presumably because the result of Ref. [25] is not close enough to the universal limit, and this points to the strong dependence $\bar{a}_3(\bar{a}_2)$ at $\bar{a}_2 \rightarrow 0$.

V. SUMMARY AND DISCUSSION

Description of three identical spinless bosons in 2D at low energy is expected to be universal (irrespective of a particular shape of the short-range potential) and parameterless if the only significant parameter—e.g., the two-body scattering length a —is chosen as a scale. In the limit of the zero-range interactions, the two-body input completely determines the solution near the triple-collision point; therefore, contrary to the corresponding problem in 3D, an additional regularization parameter is not necessary and there are neither Thomas nor Efimov effects in 2D. Both three-body binding energies and the $(2+1)$ -scattering length are the universal constants, which are determined with high precision by the numerical solution of hyperradial equations. The calculated binding energies are in excellent agreement (within the declared accuracy) with those obtained in the momentum-space calculations [29], which underlines equivalence of two distinct approaches.

All the terms of HRE's are given by the exact analytical expressions, which derivation is based on application of the BCM and the Hellmann-Feynman-type relations, the latter are known to be useful in the calculation of the coupling terms [55]. These analytical expressions are used to obtain

the asymptotic form of the total wave function both for large and small interparticle separation; in particular, the universal dependence (49) in the vicinity of the triple-collision point with the leading term $\sim \ln^3 \rho$ and the interparticle correlations given by $\ln(x_1 x_2 x_3)$ is deduced. Furthermore, the large-hyperradius asymptotic expansions are not uniform in channel number n ; therefore, the explicit dependence on n is deduced, which reveals convergence of the eigenpotentials and coupling terms to the limiting functions of $R - \ln n = \ln(\rho/n)$ at large n . The convergence is rather slow and the next-order term ($\sim n^{-1/2}$) in the large- n expansion is periodic in n with period 3; this is displayed by observing three families of eigenpotentials and coupling terms—namely, for different $n \bmod 3$. One of the reasons for slow convergence is the long-range polarization tail $\sim e^{-2R} \sim \rho^{-4}$ of the first-channel effective potential and the same order long-range term which arises due to coupling with the upper channels. As a result, one needs to take into account a large number of HRE's to study the long-range behavior of the wave function and the next-to-leading terms of the low-energy effective-range expansion for 2+1 scattering.

In summary, universal low-energy properties of three identical two-dimensional bosons are considered within the framework of the BCM used to describe two-body interactions. The approach used is based on the solution of a system of HRE's, all the terms of which are derived in the analytical form. The derivation is quite general and can be applied to a number of problems—e.g., for three identical bosons [35] and three two-component fermions [53] in 3D. The asymptotic form of the wave function is obtained both at large and small interparticle separations. The universal values of the binding energies and the (2+1)-scattering length are found with a high precision.

APPENDIX: THREE ONE-DIMENSIONAL PARTICLES

In this Appendix, the three-body problem in 1D is considered to demonstrate general applicability of the approach used, to check the numerical accuracy, and to compare convergence of the 1D and 2D calculations. The choice is based on the well-known exact solubility of the one-dimensional N -body problem with the zero-range interactions [45,46]). As usual, the problem becomes parameterless by introducing the natural units $\hbar = m = 1$ and by choosing the potential strength to fix at unit values both the two-body binding energy, $\epsilon_2 = 1$, and the two-body scattering length, $a = 1$. The exact result for the binding energy of n identical particles in 1D [45,46] is $\epsilon_n = \frac{1}{6}n(n^2 - 1)$. One should also mention that the ground-state wave function of three identical particles is of a simple form $\Psi_{gs} = C \exp(-\sum_k |x_k|)$, where the scaled Jacobi coordinates x_i and y_i are introduced similar to the above-discussed 2D case. The solution at the threshold energy $E = -1$ determines the wave function of three particles $\Psi_{sc} = \sum_k \exp(-|x_k|) - 4 \exp(-\frac{1}{2}\sum_k |x_k|)$, which entails infiniteness of the (2+1)-scattering length or existence of the zero-energy virtual state [47].

Thereafter, the approach described in the paper is applied to calculate the three-body binding energy ϵ_3 and the (2

+1)-scattering length A of three identical particles in 1D. The wave function satisfies either the equation

$$\left[\frac{\partial^2}{\partial x^2} + \frac{\partial^2}{\partial y^2} + 2 \sum_{i=1}^3 \delta(x_i) + E \right] \Psi = 0, \quad (\text{A1})$$

where the zero-range interaction is a sum of the Dirac δ functions, or the free equation complemented by the boundary condition that can be written for the each pair of the identical particles as

$$\lim_{x \rightarrow \pm 0} \left[\frac{d}{dx} \pm 1 \right] \Psi = 0. \quad (\text{A2})$$

Similar to Sec. II B, one introduces the variables ρ and α_i and expands the wave function

$$\Psi = \rho^{-1/2} \sum_{n=1}^{\infty} f_n(\rho) \Phi_n(\alpha, \rho) \quad (\text{A3})$$

in a set of eigenfunctions $\Phi_n(\alpha, \rho)$ on a circle of constant ρ , which leads to the systems of ordinary differential equations for the functions $f_n(\rho)$ which are analogous to Eqs. (9) and (10). Eigenpotentials in these systems are defined by the solution of the eigenvalue problem on a circle, and the coupling terms are defined by the analytical expressions of the same form (29), (31), and (35) as in 2D, provided the derivatives are taken over ρ . Recall that the derivation of the analytical expressions for the coupling terms in Sec. III B is equally applicable in 1D.

For the symmetry reasons, the eigenvalue problem on a circle can be solved in the interval $0 \leq \alpha_i \leq \pi/6$ by imposing the zero boundary condition $\frac{\partial \Psi}{\partial \alpha} = 0$ at $\alpha = \pi/6$ and the boundary condition at $\alpha = 0$,

$$\lim_{\alpha \rightarrow 0} \left[\frac{d}{d\alpha} + \rho \right] \Psi = 0, \quad (\text{A4})$$

which follows from Eq. (A2). The solutions of the eigenvalue problem on a circle satisfying the equation $\left(\frac{\partial^2}{\partial \alpha^2} + \xi_n^2 \right) \Phi_n(\alpha, \rho) = 0$ take a simple form $\Phi_n(\alpha, \rho) = B_n \cos(\alpha - \pi/6) \xi_n$, where the eigenvalues $\xi_n(\rho)$ are defined by the transcendental equation

$$\xi + \rho \cot \frac{\pi}{6} \xi = 0. \quad (\text{A5})$$

Due to simple dependence $\xi(\rho)$, Eq. (A5), one can derive simple analytical expressions for the coupling terms—for example,

$$P_{nm} = \frac{\cos^4(x/2) [x(x^2 - 3)(x - 2 \sin x) - 6x^2 \cos x + 3 \sin^2 x]}{3x^2(x + \sin x)^4}, \quad (\text{A6})$$

where $x = \frac{\pi}{3} \xi_n(\rho)$, as follows from Eq. (35).

Similar to the 2D case, the numerical solution of the HRE's in the form (9) and (10) with zero-boundary conditions gives the three-body binding energy, whereas the solution at the threshold energy $E = -1$ gives the (2+1)-scattering length. In the latter case the asymptotic form of the wave

function is a product of the two-body bound-state wave function $\varphi_2(x)=\exp(-|x|)$ and the function $F=1-\frac{\sqrt{3}}{2}\frac{y}{A}$, which determines the asymptotic form of the first-channel function $f_1(\rho)=\rho^{-1/2}(1-\frac{\sqrt{3}}{2}\frac{\rho}{A})$. As shown in Table II, the calculated binding energy rapidly converges to the exact value $\epsilon_3=4$ with increasing N , whereas the calculated scattering length rapidly grows with N , which manifests infiniteness of the exact scattering length. Both ϵ_3^U and ϵ_3^L are fairly well fitted to the $a+b/N^c$ dependence with the fitted values of power $c\approx 6$ and $c\approx 4$, respectively. The fitting of the scattering-length dependence on N shows that the calculated A grows as N^3 . A better precision of the 1D calculation in comparison with the 2D one is basically due to a simple form (A4) of the eigenvalue equation that provides a better accuracy of the eigenpotentials. For both 1D and 2D calculations, the second type of truncation of the HRE's provides energies converging to the exact values from below.

TABLE II. The three-body binding energy ϵ_3 (in units of the two-body binding energy) and the (2+1)-scattering length A for identical bosons in 1D. A number of HRE's is denoted by N and the superscripts U and L mark the results obtained by solving HRE's of the form (9) and (10), respectively.

N	ϵ_3^U	ϵ_3^L	A
1	3.99934308	4.00728928	3.32000×10^2
2	3.99998993	4.00055763	7.9633×10^3
3	3.99999902	4.00013463	4.555×10^4
5	3.99999994	4.00002429	3.31×10^5
7	3.99999999	4.00000816	1.1×10^6
9	4.00000000	4.00000367	2.6×10^6
12	4.00000000	4.00000149	7.9×10^6
15	4.00000000	4.00000074	$>10^7$

- [1] A. Görlitz *et al.*, Phys. Rev. Lett. **87**, 130402 (2001).
[2] D. Rychtarik, B. Engeser, H.-C. Nägerl, and R. Grimm, Phys. Rev. Lett. **92**, 173003 (2004).
[3] D. S. Petrov, M. Holzmann, and G. V. Shlyapnikov, Phys. Rev. Lett. **84**, 2551 (2000).
[4] C. G. Bao, Y. Z. He, G. M. Huang, and T. Y. Shi, Phys. Rev. A **65**, 022508 (2002).
[5] H. F. Hess, D. A. Bell, G. P. Kochanski, D. Kleppner, and T. J. Greytak, Phys. Rev. Lett. **52**, 1520 (1984).
[6] A. I. Safonov, S. A. Vasilyev, I. S. Yasnikov, I. I. Lukashevich, and S. Jaakkola, Phys. Rev. Lett. **81**, 4545 (1998).
[7] J. Järvinen, J. Ahokas, S. Jaakkola, and S. Vasilyev, Phys. Rev. A **72**, 052713 (2005).
[8] L. W. Bruch and J. A. Tjon, Phys. Rev. A **19**, 425 (1979).
[9] T. K. Lim and P. A. Maurone, Phys. Rev. B **22**, 1467 (1980).
[10] B. J. Verhaar, J. P. H. W. van den Eijnde, M. A. J. Voermans, and M. M. J. Schaffrath, J. Phys. A **17**, 595 (1984).
[11] P. O. Fedichev, M. W. Reynolds, and G. V. Shlyapnikov, Phys. Rev. Lett. **77**, 2921 (1996).
[12] E. Nielsen and J. H. Macek, Phys. Rev. Lett. **83**, 1566 (1999).
[13] B. D. Esry, C. H. Greene, and J. P. Burke, Phys. Rev. Lett. **83**, 1751 (1999).
[14] J. H. Macek, S. Y. Ovchinnikov, and G. Gasaneo, Phys. Rev. A **73**, 032704 (2006).
[15] D. S. Petrov, Phys. Rev. A **67**, 010703(R) (2003).
[16] O. I. Kartavtsev and J. H. Macek, Few-Body Syst. **31**, 249 (2002).
[17] D. S. Petrov, Phys. Rev. Lett. **93**, 143201 (2004).
[18] M. Wouters, J. Tempere, and J. T. Devreese, Phys. Rev. A **68**, 053603 (2003).
[19] Z. Idziaszek and T. Calarco, Phys. Rev. A **71**, 050701(R) (2005).
[20] C. Mora, R. Egger, and A. O. Gogolin, Phys. Rev. A **71**, 052705 (2005).
[21] V. A. Yurovsky, A. Ben-Reuven, and M. Olshanii, Phys. Rev. Lett. **96**, 163201 (2006).
[22] F. Cabral and L. W. Bruch, J. Chem. Phys. **70**, 4669 (1979).
[23] E. Nielsen, D. V. Fedorov, and A. S. Jensen, Few-Body Syst. **27**, 15 (1999).
[24] L. Vranješ and S. Kilić, Phys. Rev. A **65**, 042506 (2002).
[25] S. K. Adhikari, A. Delfino, T. Frederico, and L. Tomio, Phys. Rev. A **47**, 1093 (1993).
[26] S. K. Adhikari and W. G. Gibson, Phys. Rev. A **46**, 3967 (1992).
[27] A. D. Klemm and S. Y. Larsen, Few-Body Syst. **9**, 123 (1990).
[28] L. Platter, H.-W. Hammer, and U.-G. Meißner, Few-Body Syst. **35**, 169 (2004).
[29] H.-W. Hammer and D. T. Son, Phys. Rev. Lett. **93**, 250408 (2004).
[30] J. G. Dash, Phys. Rep., Phys. Lett. **38**, 177 (1978).
[31] Y. Kagan, G. V. Shlyapnikov, I. A. Vartanyantz, and N. A. Glukhov, Pis'ma Zh. Eksp. Teor. Fiz. **35**, 386 (1999) [JETP Lett. **35**, 477 (1982)].
[32] L. P. H. de Goeij, H. T. C. Stoof, J. M. V. A. Koelman, B. J. Verhaar, and J. T. M. Walraven, Phys. Rev. B **38**, 11500 (1988).
[33] J. H. Macek, S. Ovchinnikov, and G. Gasaneo, Phys. Rev. A **72**, 032709 (2005).
[34] D. V. Fedorov and A. S. Jensen, Phys. Rev. Lett. **71**, 4103 (1993).
[35] O. I. Kartavtsev, Few-Body Syst., Suppl. **10**, 199 (1999).
[36] E. Braaten and H.-W. Hammer, Phys. Rev. A **67**, 042706 (2003).
[37] B. Simon, Ann. Phys. (N.Y.) **97**, 279 (1976).
[38] D. Blume, Phys. Rev. B **72**, 094510 (2005).
[39] K. Wódkiewicz, Phys. Rev. A **43**, 68 (1991).
[40] Y. N. Demkov and V. N. Ostrovskii, *Zero-Range Potentials and their Applications in Atomic Physics* (Plenum Press, New York, 1988).
[41] Z. Idziaszek and T. Calarco, Phys. Rev. Lett. **96**, 013201 (2006).
[42] K. Kanjilal and D. Blume, Phys. Rev. A **73**, 060701(R) (2006).
[43] J. H. Macek, J. Phys. B **1**, 831 (1968).

- [44] E. Nielsen, D. V. Fedorov, and A. S. Jensen, *Phys. Rev. A* **56**, 3287 (1997).
- [45] J. B. McGuire, *J. Math. Phys.* **5**, 622 (1964).
- [46] E. H. Lieb and W. Liniger, *Phys. Rev.* **130**, 1605 (1963).
- [47] A. Amaya-Tapia, S. Y. Larsen, and J. Popiel, *Few-Body Syst.* **23**, 87 (1998).
- [48] D. Bollé and F. Gesztesy, *Phys. Rev. A* **30**, 1279 (1984).
- [49] B. J. Verhaar, L. P. H. de Goeij, J. P. H. W. van den Eijnde, and E. J. D. Vredenburg, *Phys. Rev. A* **32**, 1424 (1985).
- [50] A. F. Starace and G. L. Webster, *Phys. Rev. A* **19**, 1629 (1979).
- [51] H. T. Coelho and J. E. Hornos, *Phys. Rev. A* **43**, 6379 (1991).
- [52] H. Bateman and A. Erdélyi, *Higher Transcendental Functions* (McGraw-Hill, New York, 1953).
- [53] O. I. Kartavtsev and A. V. Malykh (unpublished).
- [54] T. F. O'Malley, L. Spruch, and L. Rosenberg, *J. Math. Phys.* **2**, 491 (1961).
- [55] A. V. Stolyarov and M. S. Child, *Phys. Rev. A* **63**, 052510 (2001).